Chinese Journal of
POLYMER SCIENCE

RESEARCH ARTICLE

https://doi.org/10.1007/s10118-023-3026-z
Chinese J. Polym. Sci. **2023**, *41*, 1584–1590

n-Type Semiconductive Polymers Based on Pyrene-1,5,6,10-Tetracarboxyl Diimide

Xu-Dong Bai, Zi-Di Yu, Yao Li, Tian-Yu Zhang, Di Zhang, Jie-Yu Wang, Jian Pei*, and Da-Hui Zhao*

Beijing National Laboratory for Molecular Sciences, Centre of Soft Matter Science and Engineering and Key Lab of Polymer Chemistry & Physics of Ministry of Education, College of Chemistry, Peking University, Beijing 100871, China

Electronic Supplementary Information

Abstract Donor-acceptor (D-A) conjugated polymers comprising electron-deficient aromatic dicarboximide units represent an important type of organic semiconductors, especially for electron transporting properties. Pyrene-1,5,6,10-tetracarboxyl diimide (PyDI), a new PAH dicarboximide molecule recently reported by us, provides a fine balance between the electron-stabilizing ability and π-stacking tendency, as compared to the naphthalenediimide (NDI) and perylenediimide (PDI) analogues. In this study, using thienylene-vinylene-thienylene (TVT) and biselenophene (BS) as the electron donating comonomer, along with PyDI as the acceptor moiety, we develop two new D-A type conjugated polymers, which exhibit impressive electron-transporting performance. Specifically, in the solution-processed OFET devices, electron mobility of 0.18 and 0.20 $cm^2 \cdot V^{-1} \cdot s^{-1}$ are achieved with these polymers, respectively. Such findings further prove the optimal potential of PyDI for application as an electron-acceptor building block in the development of polymeric *n*-type semiconductors among all various high-performance functional D-A polymers.

Keywords Pyrenediimide; Conjugated polymers; Donor-acceptor; Organic electronics

Citation: Bai, X. D.; Yu, Z. D.; Li, Y.; Zhang, T. Y.; Zhang, D.; Wang, J. Y.; Pei, J.; Zhao, D. H. *n*-Type semiconductive polymers based on pyrene-1,5,6,10-tetracarboxyl diimide. *Chinese J. Polym. Sci.* **2023**, *41*, 1584–1590.

INTRODUCTION

Over the past few decades, conjugated polymers have attracted significant attention due to their unique optoelectronic properties and excellent solution-processing features, facilitating their application as promising candidates for the next generation of semiconductive materials.[1–3] Compared to small molecules, polymers possess superior mechanical properties. Moreover, benefitted from the slow chain dynamics of macromolecules, a suitable balance is possibly attained between morphological stability and material crystallinity, thus promoting more favorable device performance.[4] Through the studies of a wide range of chemical structures, conjugated polymers of D-A type backbones stand out and now play a valuable role in the research of organic electronics, for offering readily tunable electronic properties and lower inter-chain charge transport barriers due to efficient electronic coupling.[5–10] However, the functional performance and structural diversity of *n*-type polymer semiconductors still lag behind the *p*-type analogues.[11–15] The disadvantaged properties for the former partially result from the far fewer available electron-accepting units, which is entangled with the greater difficulties encountered in the syntheses and chemical modifications with the electron-deficient aromatic structures.

Polycyclic aromatic dicarboximides (PAIs) featuring multiple highly electron-withdrawing groups around the periphery of aromatic cores are widely used acceptor repeating units in conjugated D-A polymers,[16–19] as represented by naphthalenediimide (NDI) and perylenediimide (PDI).[20–22] A distinctive example that has received vast attention is N2200,[23,24] for exhibiting superior device performance in various application scenarios by virtue of its excellent optical and electronic properties.[25] As an attempt to further diversify the structural pool of PAIs, we previously developed a new molecule utilizing the pyrene skeleton, namely pyrene-1,5,6,10-tetracarboxyl diimide (PyDI).[26] With a mid-sized aromatic core, PyDI demonstrates pronounced electron-withdrawing effect similar to NDI, with slightly tempered aromatic stacking tendency as compared to larger PDI. Such a molecular design is expected to produce improved charge transport capabilities under facile solution-processing conditions. Unlike the other regio-isomers of pyrene diimides reported in the prior work,[27–30] PyDI features two six-membered dicarboximide rings fused to the pyrene moiety, which are known to bestow superior functional properties, including high sta-

* Corresponding authors, E-mail: jianpei@pku.edu.cn (J.P.)
E-mail: dhzhao@pku.edu.cn (D.H.Z.)

Special Issue: Celebrating the 70th Anniversary of the Establishment of Polymer Program at Peking University
Received April 28, 2023; Accepted July 4, 2023; Published online August 7, 2023

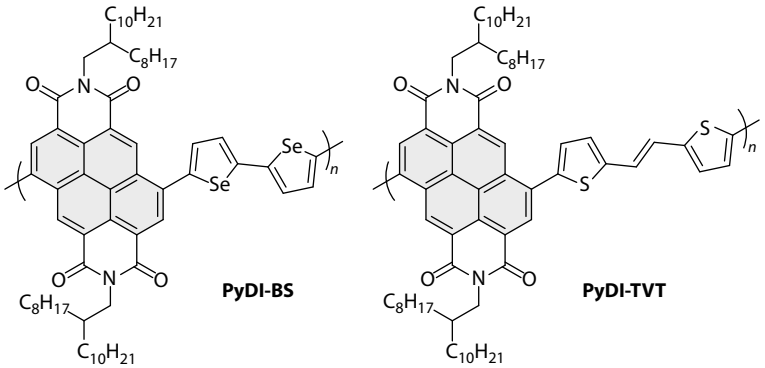

Fig. 1 Chemical structures of new PyDI polymers studied in this work.

bility, low electron-injection barrier, optimal radical anion stability, and favorable rotational and slipping packing geometry.[31,32] The two previously studied conjugated D-A copolymers, **PyDI-T** and **PyDI-TT**,[26] both exhibited impressive *n*-type semiconductive ability, illustrating the potential of PyDI in constructing high-performance electron-transporting polymer materials.

In this study, we further synthesize two new D-A conjugated polymers, **PyDI-TVT** and **PyDI-BS** (Fig. 1). By employing different comonomers to coordinate with PyDI, we expected to modulate the inter-chain interactions and improve the electron transport capability of the polymers. Stille cross-coupling reaction is used to couple the more electron-rich thienylene-vinylene-thienylene (TVT) and biselenophene (BS) units with PyDI. The introduction of TVT unit presumably enhances the planarity of the polymer backbone, by restricting the rotation of thiophene rings, and thus further promotes the long-range order of chain packing.[33–35] This speculation is confirmed by the density functional theory (DFT) calculations. On the other hand, the incorporation of the more electron-donating biselenophene is designed to improve the orbital overlap and increase the charge carrier mobility.[36,37] Additionally, the stronger chalcogen-chalcogen interactions caused by the larger p-orbitals of selenium atoms may as well enhance the inter-chain interactions of polymers.[38–41] The molecular designs are found to favour both electron-transport and light-absorbing abilities, by inducing more significant intramolecular charge-transfer characters. In the polymer-based OFET devices, **PyDI-TVT** and **PyDI-BS** both show optimal semiconducting performance, with electron mobilities up to 0.18 and 0.20 $cm^2 \cdot V^{-1} \cdot s^{-1}$ achieved, respectively. These results not only demonstrate the application potentials of the new conjugated polymers, but also further prove PyDI to be a useful new PAI unit in the development of organic electronic materials.

EXPERIMENTAL

General Methods

All the reactions involving air- or moisture-sensitive compounds were carried out in dry reaction vessels under inert atmosphere. All solvents and reagents were purchased from commercial sources and used without further purification unless otherwise noted. Toluene was dried over sodium and distilled prior to use. 3,8-Dibromo-1,5,6,10-PyDI (**diBr-PyDI**) was prepared following the previously reported method.[26] The synthesis of 5,5'-bis(trimethylstannyl)-2,2'-biselenophene was referenced to the literature procedures.[42]

Synthesis of PyDI-TVT

A Schlenk tube charged with **diBr-PyDI** (41.6 mg, 0.0393 mmol), (*E*)-1,2-bis(5-(trimethylstannyl)thiophen-2-yl)ethene (20.5 mg, 0.0396 mmol), $Pd_2(dba)_3$ (2.1 mg, 0.0023 mmol), and P(*o*-tol)$_3$ (2.8 mg, 0.0091 mmol) was evacuated and back-filled with nitrogen three times, and then toluene (1 mL) was added *via* a syringe under nitrogen atmosphere. The reaction vessel was sealed and stirred at 110 °C for 60 h. Upon cooling to room temperature, the polymer was precipitated by dispersing the reaction mixture in methanol (50 mL). The obtained deep green solid was transferred to a Soxhlet apparatus. The crude product was subjected to sequential Soxhlet extractions with methanol, hexane and chloroform. After extraction with chloroform, the polymer solution was concentrated to ~2 mL, and then dripped into methanol (50 mL) with stirring. The precipitates were collected by filtration, washed with methanol, and dried under reduced pressure to give **PyDI-TVT** (38 mg, 88%) as a deep green solid. ^{1}H-NMR (400 MHz, $CDCl_3$, δ, ppm): 9.57–9.23 (m, 2H), 8.89 (br, 2H), 7.62–7.19 (m, 6H), 4.23 (br, 4H), 2.07 (br, 2H), 1.51–1.03 (m, 64H), 0.91–0.78 (m, 12H). HT-GPC: M_n=21.2 kDa, M_w=53.0 kDa, PDI=2.50.

Synthesis of PyDI-BS

The polymer was prepared from **diBr-PyDI** (35.2 mg, 0.0332 mmol) and 5,5'-bis(trimethylstannyl)-2,2'-biselenophene (19.5 mg, 0.0333 mmol) *via* a procedure similar with that used for synthesizing **PyDI-TVT**. **PyDI-BS** (35 mg, 91%) was obtained as a deep green solid. ^{1}H-NMR (400 MHz, $CDCl_3$, δ, ppm): 9.40 (br, 2H), 8.90 (br, 2H), 8.00–7.35 (m, 4H), 4.29 (br, 4H), 2.09 (br, 2H), 1.51–1.07 (m, 64H), 0.91–0.75 (m, 12H). HT-GPC: M_n=57.7 kDa, M_w=215.3 kDa, PDI=3.73.

Device Fabrication and Characterization

The devices were fabricated with a conventional top-gate/bottom-contact (TG/BC) configuration. The patterned Au/SiO_2/Si substrates were immersed in a phenylethanethiol solution (5 mmol/L in anhydrous toluene) for 4 h to form the self-assembled monolayers, followed by washing with anhydrous toluene and isopropyl alcohol. The semiconducting layer was then deposited by spin-coating the polymer solution onto the patterned Au/SiO_2/Si substrate with SAM at 1500 r/min, followed by thermal annealing at 180 °C for 5 min. A CYTOP solution was spin-coated as the dielectric layer. Before

https://doi.org/10.1007/s10118-023-3026-z

thermal annealing at 100 °C for 1 h, an aluminum layer deposited *via* thermal evaporation as the gate electrode. The devices were characterized in the air with an Agilent B2912A Semiconductor Analyzer. The electron mobility in the saturation region was calculated according to the following equation: $I_D = (W/2L)\, C_i\mu(V_G - V_T)^2$, where I_D is the drain current, W and L are the device channel width and length, C_i is the gate dielectric layer capacitance per unit area, μ is the carrier mobility, and V_G and V_T are gate voltage and threshold voltage, respectively.

RESULTS AND DISCUSSION

Polymer Syntheses and Characterizations

The synthetic routes of polymers **PyDI-TVT** and **PyDI-BS** are shown in Scheme 1. The detailed experimental procedures are provided in the experimental section. Both polymers can be prepared efficiently *via* Stille coupling reactions from **diBr-PyDI** and relevant comonomers, and obtained as dark green solids with a glossy appearance. The molecular weights (MWs) of the polymers are determined to be 21.2 and 51.7 kDa, respectively, by the high-temperature gel permeation chromatography (HT-GPC, Fig. S1 in the electronic supplementary information, ESI). The polymers exhibit good solubility in chloroform. The relatively high molecular weight is apparently necessary for the formation of ordered crystalline domains in the film state, which is crucial to attaining desirable carrier mobility.[43,44] The TGA results from both polymers **PyDI-TVT** and **PyDI-BS** reveal their good thermal stability with high decomposition temperature of 434 and 438 °C, respectively (Figs. S2 and S3 in ESI).

Optical and Electrochemical Properties

The UV-Vis-NIR absorption spectra of **PyDI-TVT** and **PyDI-BS** in dilute chloroform solution (1×10^{-5} mol/L) and the thin-film state are shown in Fig. 2(a), and the relevant data are listed in Table 1. Both **PyDI-TVT** and **PyDI-BS** depict a long-wavelength absorption band in solution, with maxima observed at around 690 and 669 nm, respectively. The broad low-energy bands indicate efficient conjugation and charge-transfer features between the donor and acceptor moieties in the polymer backbone. Notably, while the two polymers exhibit similar extinction coefficient values in the low energy region with those shown by **PyDI-T** and **PyDI-TT** reported previously,[26] the absorption peaks of **PyDI-TVT** and **PyDI-BS** are bathochromic shifted by *ca*. 40 and 20 nm, respectively, compared to that of **PyDI-TT** (Figs. S6 and S7 in ESI). These results also suggest the better electron-donating abilities of TVT and BS units. In the thin-film state, moderate band gap narrowing and band shape broadening as compared to the solution state are shown by both polymers, with evident absorption tails reaching over 1000 nm. Based on the absorption onset of the polymer films, the optical band gaps are estimated to be 1.54 and 1.59 eV for **PyDI-TVT** and **PyDI-BS**, respectively.

To investigate the redox behaviors of the polymers, electrochemical characterizations are conducted, with which the LUMO energy levels of **PyDI-TVT** and **PyDI-BS** are determined to be at −3.73 and −3.75 eV, respectively (Fig. 2b and Figs. S4 and S5 in ESI). Combined with the corresponding optical bandgap values from the absorption spectra, the HOMO energy levels of the two polymers are calculated to be around −5.27 and −5.34 eV. By comparing the MO energy level data of all four PyDI polymers, the results suggest that the LUMO of the polymers are mainly determined by the electron-accepting unit of PyDI, while the stronger electron-pushing ability of the donor units in the newly synthesized polymers appear to slightly raise the HOMO levels as compared to those

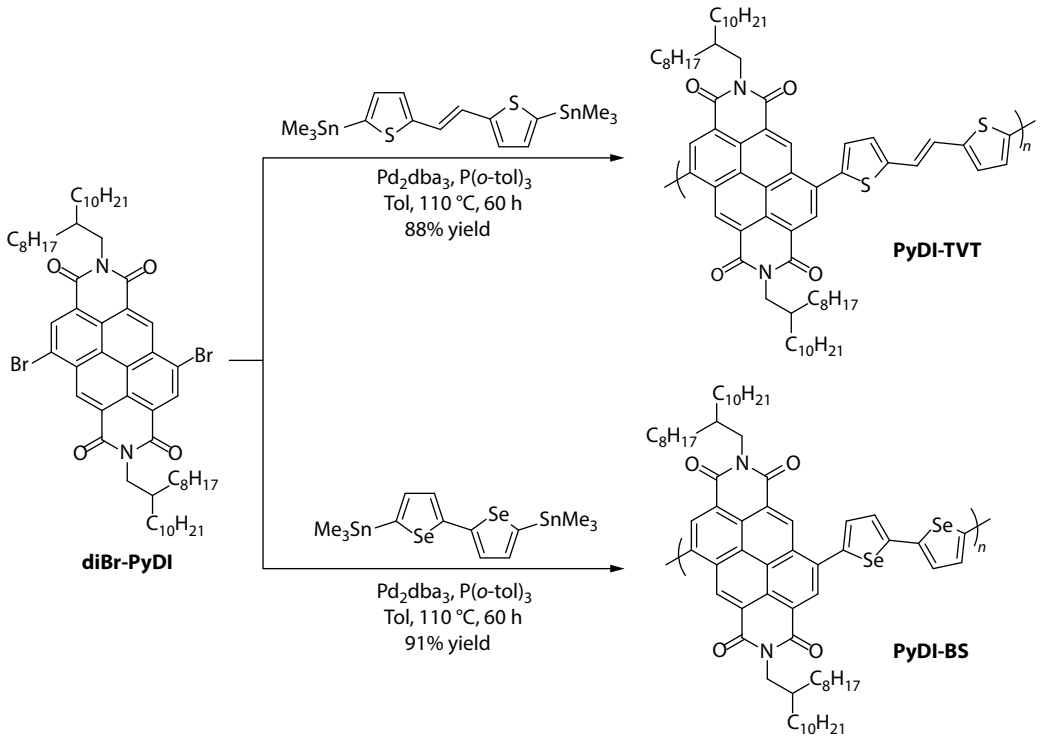

Scheme 1 Synthesis routes to **PyDI-TVT** and **PyDI-BS**.

https://doi.org/10.1007/s10118-023-3026-z

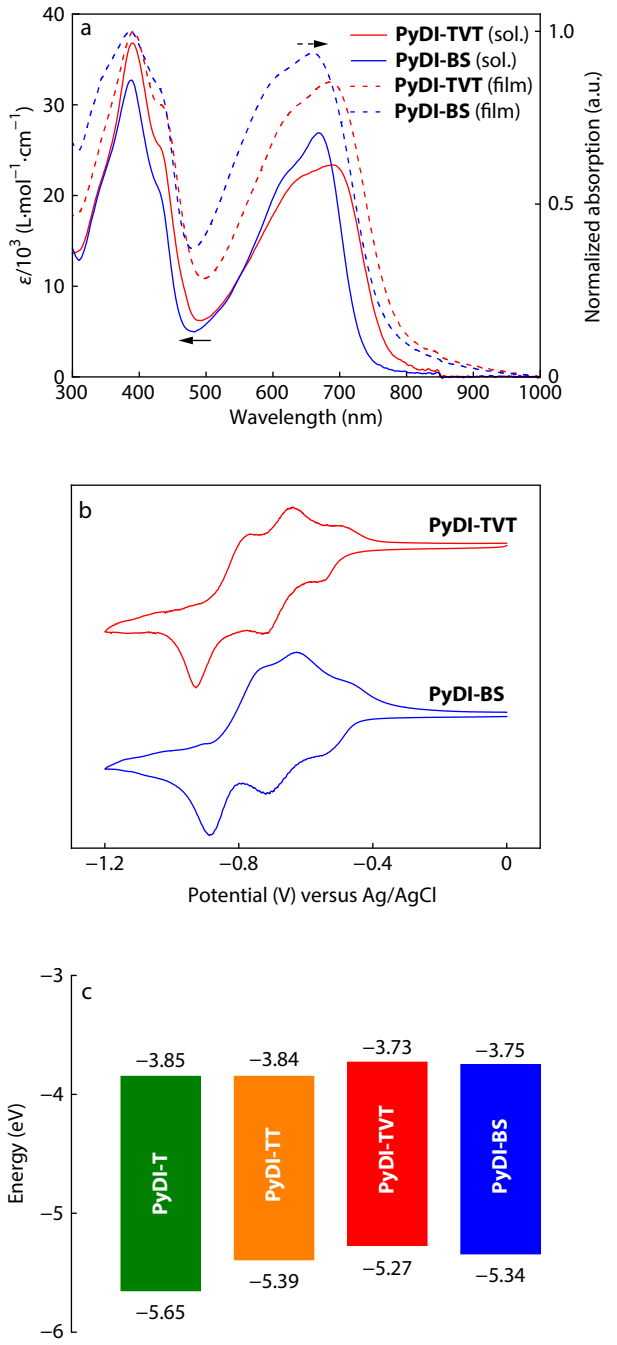

Fig. 2 (a) Absorption spectra of **PyDI-TVT** and **PyDI-BS** in chloroform (1×10^{-5} mol/L) and thin films; (b) Cyclic voltammograms of the polymers; (c) FMO energy levels of **PyDI-TVT** and **PyDI-BS** in comparison to **PyDI-T** and **PyDI-TT** (E_{LUMO} is determined by CV and E_{HOMO} is estimated from E_{LUMO} and optical band gap).

of **PyDI-T** and **PyDI-TT** (Fig. 2c).

Theoretical Investigations

Density functional theory (DFT) calculations are then conducted at the B3LYP/6-31G(d,p) level to gain insights into the molecular geometry and frontier orbital features of **PyDI-TVT** and **PyDI-BS**. Tetramers are used as models to simulate the backbone conformation of the polymers, and the branched alkyl chains are replaced here with methyl groups in the calculations. The optimized backbone conformations of **PyDI-TVT** and **PyDI-BS** show dihedral angles of approximately 40° and 43°, respectively, between the PyDI and donor units (Figs. 3a and 3b). These values are comparable to the dihedral angles calculated for **PyDI-T** (~42°) and **PyDI-TT** (~40°), while smaller than that of N2200 (~50°).[26] These data suggest that both new polymers have relatively flat backbones, potentially leading to more effective conjugation and efficient electron transport.

The HOMOs in both **PyDI-TVT** and **PyDI-BS** are demonstrated to be delocalized over a couple of repeat units, while in contrast LUMOs are more localized with the electron-deficient PyDI segments (Figs. 3c and 3d). Furthermore, time-dependent DFT (TD-DFT) calculation results at the B3LYP/6-311+G(d,p) level agree well with the experimentally observed absorption properties of both polymers, confirming that the low-energy absorption bands are mainly attributable to the transition of $S_0 \rightarrow S_1$ (Figs. S9 and S11 in ESI). The electron and hole distribution equivalence surfaces of the excited states are analyzed by Multifwn[45] and reveal that, for the excited states of both polymers, holes are almost completely distributed over the donor units, while electrons are mainly located with the PyDI units, implying significant charge separation features (Figs. S10 and S12 in ESI).

Field-Effect Transistor Characterizations

To investigate the charge transport properties of two new polymers, OFETs with the TG/BC configuration are prepared. By the top-gate dielectric layer, the active layer of solution-cast polymer is well protected from the moisture and oxygen, allowing the devices to operate with stability in the air. The transfer and output characteristics of **PyDI-TVT** and **PyDI-BS** are shown in Fig. 4 and Table S1 in ESI, in which all OFET devices exhibit the typical unipolar *n*-channel field-effect behaviors. After annealing at 180 °C, the thin films of **PyDI-TVT** and **PyDI-BS** achieve the impressive electron mobility values of up to 0.18 and 0.20 $cm^2 \cdot V^{-1} \cdot s^{-1}$, respectively, while showing decent current I_{on}/I_{off} modulation (10^4–10^5). Such magnitudes of mobility are close to that accomplished by **PyDI-TT**, further approving the efficacy of PyDI-based conjugated polymers in serving as semiconductive materials.

Morphological Studies

To further examine the surface morphology of the polymer thin

Table 1 Optical and electrochemical property data.

Polymer	M_n/M_w (kDa)	T_{dec} (°C)	$\lambda_{max,sol}$ [a] (nm)	$\lambda_{max,film}$ (nm)	$E_{g,opt}$ [b] (eV)	E_{LUMO} [c] (eV)	E_{HOMO} [d] (eV)
PyDI-TVT	21.2/53.0	434	690	688	1.54	−3.73	−5.27
PyDI-BS	57.7/215.3	438	669	668	1.59	−3.75	−5.34

[a] Measured in chloroform solution (1×10^{-5} mol/L); [b] Calculated from the absorption onset in thin films for polymers; [c] Determined using CV; [d] Estimated from $E_{HOMO} = E_{LUMO} - E_{g,opt}$.

https://doi.org/10.1007/s10118-023-3026-z

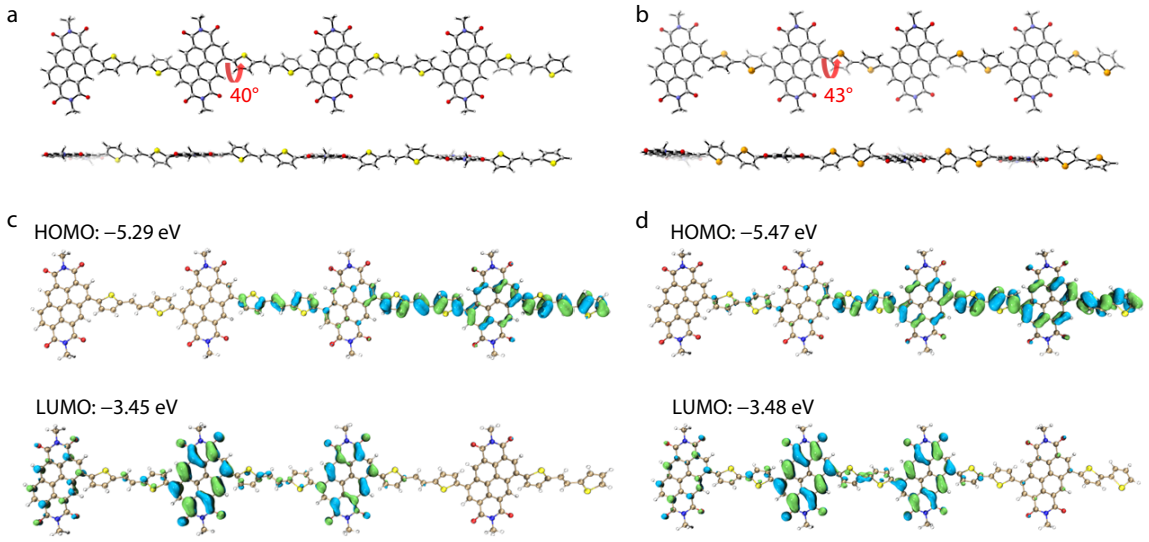

Fig. 3 DFT optimized geometry (a and b) and electronic structures (c and d) of the tetramer models of polymers **PyDI-TVT** (a and c) and **PyDI-BS** (b and d).

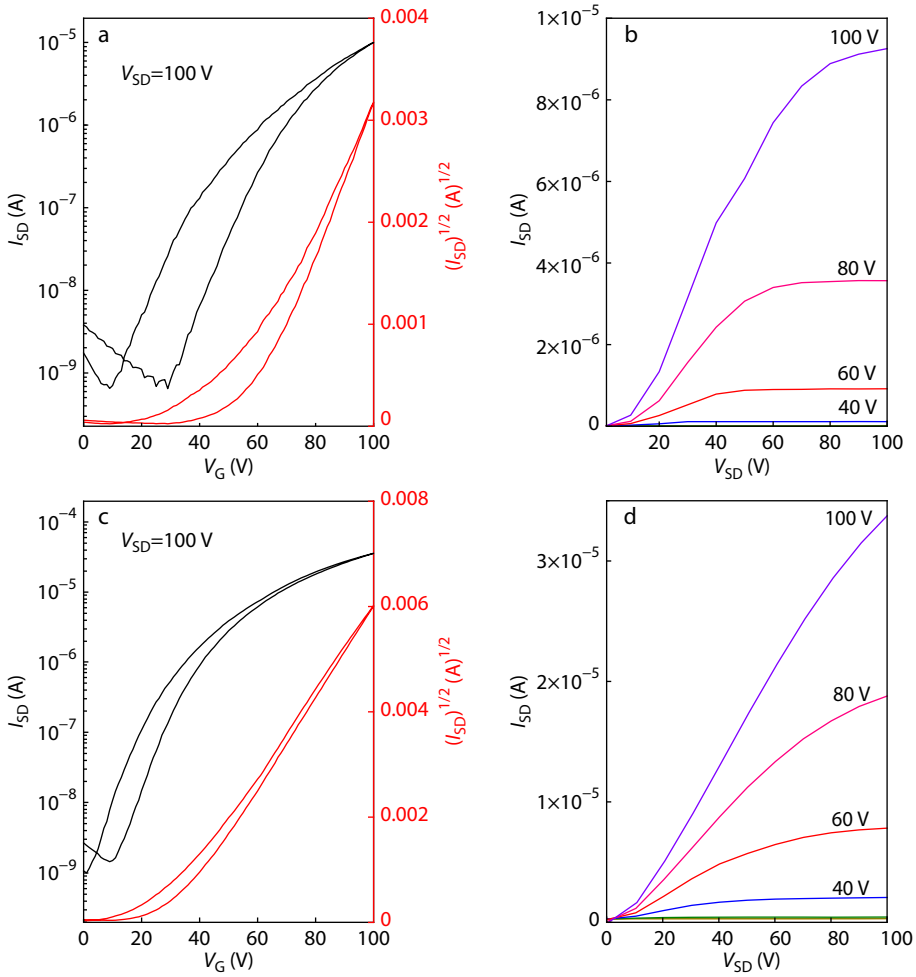

Fig. 4 Transfer (a and c) and output characteristics (b and d) of TG/BC OFET devices fabricated with **PyDI-TVT** (a and b) and **PyDI-BS** (c and d).

films, the tapping mode atomic force microscopy (AFM) and grazing-incidence wide-angle X-ray scattering (GIWAXS) techniques are used for analyses. As shown in Fig. 5(a), the **PyDI-BS** film exhibits fibrous surface morphology, revealing highly ordered organization of the nanostructures. However, the **PyDI-TVT** film (Fig. 5b) manifests amorphous morphology

https://doi.org/10.1007/s10118-023-3026-z

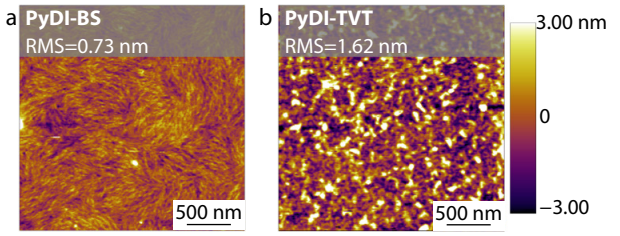

Fig. 5 AFM height images of (a) **PyDI-BS** and (b) **PyDI-TVT** thin films prepared under the same conditions as applied to OFET fabrications, with an annealing temperature of 180 °C.

with a rougher surface, which likely accounts for the greater hysteresis shown by the polymer in the OFET devices. The 2D-GIWAXS patterns and corresponding 1D out-of-plane and in-plane scattering profiles are provided in the ESI (Figs. S14 and S15 in ESI). For **PyDI-TVT** and **PyDI-BS**, the polymer *d-d* distances calculated from the (100) diffraction peaks are 22.5 Å and 23.1 Å, respectively, while the *π-π* stacking distances are both 3.8 Å, based on the (010) peaks. These values are similar with those observed with **PyDI-TT**, suggesting that similar degrees of lamellar stacking exist in these polymer thin films. **PyDI-BS** exhibits a greater extent of edge-on orientation compared to **PyDI-TVT**, which is generally more favorable to efficient electron transport according to the conventional charge-hoping theory.[46]

CONCLUSIONS

In the current work, we aim to further demonstrate the electron-transporting capability of polymers based on the PyDI acceptor unit, by synthesizing two new materials, **PyDI-TVT** and **PyDI-BS**. These polymers are designed for optimizing the inter-chain interactions, as the TVT unit is potentially capable of improving the backbone planarity and thus chain-packing order in thin films, while the BS unit may enhance the inter-chain forces by introducing the selenium-selenium interactions. The *n*-type semiconductor properties of the materials are characterized by OFET devices fabricated by using the polymers as the active layer, which demonstrate good electron mobility up to 0.20 $cm^2 \cdot V^{-1} \cdot s^{-1}$. The results herein further highlight the promising value of PyDI unit as a new potent electron-deficient building block applicable to the development of high-performance organic semiconductive materials.

Conflict of Interests

The authors declare no interest conflict.

Electronic Supplementary Information

Electronic supplementary information (ESI) is available free of charge in the online version of this article at http://doi.org/10.1007/s10118-023-3026-z.

ACKNOWLEDGMENTS

This work was financially supported by the National Natural Science Foundation of China (Nos. 21925501, 22175004 and 22020102001) and the Beijing National Laboratory for Molecular Sciences (No. BNLMS-CXXM-201902). Part of the characterization measurements were performed at the Analytical Instrumentation Center of Peking University, and the computational resources were supplied by the High-performance Computing Platform of Peking University.

REFERENCES

1 Wang, C.; Dong, H.; Hu, W.; Liu, Y.; Zhu, D. Semiconducting pi-conjugated systems in field-effect transistors: a material odyssey of organic electronics. *Chem. Rev.* **2012**, *112*, 2208–2267.
2 Liu, C.; Wang, K.; Gong, X.; Heeger, A. J. Low bandgap semiconducting polymers for polymeric photovoltaics. *Chem. Soc. Rev.* **2016**, *45*, 4825–4846.
3 Facchetti, A. *π*-Conjugated polymers for organic electronics and photovoltaic cell applications. *Chem. Mater.* **2010,** *23*, 733–758.
4 Beaujuge, P. M.; Reynolds, J. R. Color control in *π*-conjugated organic polymers for use in electrochromic devices. *Chem. Rev.* **2010**, *110*, 268–320.
5 Li, Y. F.; Guo, Y. L.; Liu, Y. Q. Recent progress in donor-acceptor type conjugated polymers for organic field-effect transistors. *Chinese J. Polym. Sci.* **2023**, *41*, 652–670.
6 Kim, M.; Ryu, S. U.; Park, S. A.; Choi, K.; Kim, T.; Chung, D.; Park, T. Donor–acceptor-conjugated polymer for high-performance organic field-effect transistors: a progress report. *Adv. Funct. Mater.* **2019**, *30*, 1904545.
7 Yin, B.; Chen, Z.; Pang, S.; Yuan, X.; Liu, Z.; Duan, C.; Huang, F.; Cao, Y. The renaissance of oligothiophene-based donor-acceptor polymers in organic solar cells. *Adv. Energy Mater.* **2022**, *12*, 2104050.
8 Moser, M.; Savva, A.; Thorley, K.; Paulsen, B. D.; Hidalgo, T. C.; Ohayon, D.; Chen, H.; Giovannitti, A.; Marks, A.; Gasparini, N.; Wadsworth, A.; Rivnay, J.; Inal, S.; McCulloch, I. Polaron delocalization in donor-acceptor polymers and its impact on organic electrochemical transistor performance. *Angew. Chem. Int. Ed.* **2021**, *60*, 7777–7785.
9 Wen, K.; Tan, H.; Peng, Q.; Chen, H.; Ma, H.; Wang, L.; Peng, A.; Shi, Q.; Cai, X.; Huang, H. Achieving efficient NIR-II type-I photosensitizers for photodynamic/photothermal therapy upon regulating chalcogen elements. *Adv. Mater.* **2022**, *34*, 2108146.
10 Tan, Z. R.; Xing, Y. Q.; Cheng, J. Z.; Zhang, G.; Shen, Z. Q.; Zhang, Y. J.; Liao, G.; Chen, L.; Liu, S. Y. EDOT-based conjugated polymers accessed *via* C-H direct arylation for efficient photocatalytic hydrogen production. *Chem. Sci.* **2022**, *13*, 1725–1733.
11 Sun, H.; Guo, X.; Facchetti, A. High-performance *n*-type polymer semiconductors: applications, recent development, and challenges. *Chem* **2020**, *6*, 1310–1326.
12 Tang, H.; Liang, Y.; Liu, C.; Hu, Z.; Deng, Y.; Guo, H.; Yu, Z.; Song, A.; Zhao, H.; Zhao, D.; Zhang, Y.; Guo, X.; Pei, J.; Ma, Y.; Cao, Y.; Huang, F. A solution-processed n-type conducting polymer with ultrahigh conductivity. *Nature* **2022**, *611*, 271–277.
13 Jia, T.; Zhang, J.; Zhong, W.; Liang, Y.; Zhang, K.; Dong, S.; Ying, L.; Liu, F.; Wang, X.; Huang, F.; Cao, Y. 14.4% efficiency all-polymer solar cell with broad absorption and low energy loss enabled by a novel polymer acceptor. *Nano Energy* **2020,** *72*, 104718.
14 Dong, C.; Deng, S.; Meng, B.; Liu, J.; Wang, L. A distannylated monomer of a strong electron-accepting organoboron building block: enabling acceptor-acceptor-type conjugated polymers for n-type thermoelectric applications. *Angew. Chem. Int. Ed.* **2021**, *60*, 16184–16190.
15 He, X.; Ye, F.; Guo, J. C.; Chang, W.; Ma, B.; Ding, R.; Wang, S.; Liang, Y.; Hu, D.; Guo, Z. H.; Ma, Y. An N-oxide containing conjugated

semiconducting polymer with enhanced electron mobility *via* direct (hetero)arylation polymerization. *Polym. Chem.* **2023**, *14*, 1945–1953.
16 Feng, K.; Guo, H.; Sun, H.; Guo, X. n-Type organic and polymeric semiconductors based on bithiophene imide derivatives. *Acc. Chem. Res.* **2021,** *54*, 3804–3817.
17 Li, J.; Liu, M.; Yang, K.; Wang, Y.; Wang, J.; Chen, Z.; Feng, K.; Wang, D.; Zhang, J.; Li, Y.; Guo, H.; Wei, Z.; Guo, X. Selenium substitution in bithiophene imide polymer semiconductors enables high-performance n-type organic thermoelectric. *Adv. Funct. Mater.* **2023**, *33*, 2213911.
18 Shi, W.; Yang, X.; Li, X.; Meng, L.; Zhang, D.; Zhu, Z.; Xiao, X.; Zhao, D. Syntheses of anthracene-centered large PAH diimides and conjugated polymers. *Chem. Eur. J.* **2022**, *28*, 202104598.
19 Zhao, L.; Li, W.; Qin, H.; Yi, X.; Zeng, W.; Zhao, Y.; Chen, H. Electron-transporting conjugated polymers from novel aromatic five-membered diimides: naphtho[1,2-*b*:4,3-*b*']-dithiophene and -diselenophene diimides. *Macromolecules* **2023**, *56*, 2990–3003.
20 Kobaisi, M. A.; Bhosale, S. V.; Latham, K.; Raynor, A. M.; Bhosale, S. V. Functional naphthalene diimides: synthesis, properties, and applications. *Chem. Rev.* **2016**, *116*, 11685–11796.
21 Bhosale, S. V.; Al Kobaisi, M.; Jadhav, R. W.; Morajkar, P. P.; Jones, L. A.; George, S. Naphthalene diimides: perspectives and promise. *Chem. Soc. Rev.* **2021**, *50*, 9845–9998.
22 Zhan, X.; Facchetti, A.; Barlow, S.; Marks, T. J.; Ratner, M. A.; Wasielewski, M. R.; Marder, S. R. Rylene and related diimides for organic electronics. *Adv. Mater.* **2011**, *23*, 268–284.
23 Kim, Y. J.; Kim, N. K.; Park, W. T.; Liu, C.; Noh, Y. Y.; Kim, D. Y. Kinetically controlled crystallization in conjugated polymer films for high-performance organic field-effect transistors. *Adv. Funct. Mater.* **2019**, *29*, 1807786.
24 Bucella, S. G.; Luzio, A.; Gann, E.; Thomsen, L.; McNeill, C. R.; Pace, G.; Perinot, A.; Chen, Z.; Facchetti, A.; Caironi, M. Macroscopic and high-throughput printing of aligned nanostructured polymer semiconductors for MHz large-area electronics. *Nat. Commun.* **2015**, *6*, 8394.
25 Sun, H.; Wang, L.; Wang, Y.; Guo, X. Imide-functionalized polymer semiconductors. *Chem. Eur. J.* **2019**, *25*, 87–105.
26 Li, Y.; Yao, Z.; Xie, J.; Han, H.; Yang, G.; Bai, X.; Pei, J.; Zhao, D. Pyrene-1,5,6,10-tetracarboxyl diimide: a new building block for high-performance electron-transporting polymers. *J. Mater. Chem. C* **2021**, *9*, 7599–7606.
27 Zou, L.; Wang, X. Y.; Zhang, X. X.; Dai, Y. Z.; Wu, Y. D.; Wang, J. Y.; Pei, J. Toward electron-deficient pyrene derivatives: construction of pyrene tetracarboxylic diimide containing five-membered imide rings. *Chem. Commun.* **2015**, *51*, 12585–12588.
28 Zhao, D.; Wu, Q.; Cai, Z.; Zheng, T.; Chen, W.; Lu, J.; Yu, L. Electron acceptors based on α-substituted perylene diimide (PDI) for organic solar cells. *Chem. Mater.* **2016**, *28*, 1139–1146.
29 Wu, Z. H.; Huang, Z. T.; Guo, R. X.; Sun, C. L.; Chen, L. C.; Sun, B.; Shi, Z. F.; Shao, X.; Li, H.; Zhang, H. L. 4,5,9,10-Pyrene diimides: a family of aromatic diimides exhibiting high electron mobility and two-photon excited emission. *Angew. Chem. Int. Ed.* **2017,** *56*, 13031–13035.
30 Zindy, N.; Aumaitre, C.; Mainville, M.; Saneifar, H.; Johnson, P. A.; Bélanger, D.; Leclerc, M. Pyrene diimide based π-conjugated copolymer and single-walled carbon nanotube composites for lithium-ion batteries. *Chem. Mater.* **2019**, *31*, 8764–8773.
31 Sanyal, S.; Manna, A. K.; Pati, S. K. Effect of imide functionalization on the electronic, optical, and charge transport properties of coronene: a theoretical study. *J. Phys. Chem. C* **2013**, *117*, 825–836.
32 Chen, X. K.; Zou, L. Y.; Guo, J. F.; Ren, A. M. An efficient strategy for designing n-type organic semiconductor materials—introducing a six-membered imide ring into aromatic diimides. *J. Mater. Chem.* **2012**, *22*, 6471.
33 Kim, R.; Amegadze, P. S. K.; Kang, I.; Yun, H. J.; Noh, Y.-Y.; Kwon, S. K.; Kim, Y. H. High-mobility air-stable naphthalene diimide-based copolymer containing extended π-conjugation for n-channel organic field effect transistors. *Adv. Funct. Mater.* **2013**, *23*, 5719–5727.
34 Sung, M. J.; Luzio, A.; Park, W. T.; Kim, R.; Gann, E.; Maddalena, F.; Pace, G.; Xu, Y.; Natali, D.; de Falco, C.; Dang, L.; McNeill, C. R.; Caironi, M.; Noh, Y. Y.; Kim, Y. H. High-mobility naphthalene diimide and selenophene-vinylene-selenophene-based conjugated polymer: n-channel organic field-effect transistors and structure-property relationship. *Adv. Funct. Mater.* **2016**, *26*, 4984–4997.
35 An, N.; Ran, H.; Geng, Y.; Zeng, Q.; Hu, J.; Yang, J.; Sun, Y.; Wang, X.; Zhou, E. Exploring a fused 2-(thiophen-2-yl)thieno[3,2-*b*]thiophene (T-TT) building block to construct n-type polymer for high-performance all-polymer solar cells. *ACS Appl. Mater. Interfaces* **2019**, *11*, 42412–42419.
36 Zade, S. S.; Zamoshchik, N.; Bendikov, M. Oligo- and polyselenophenes: a theoretical study. *Chem. Eur. J.* **2009**, *15*, 8613–8624.
37 Tsai, C. E.; Yu, R. H.; Lin, F. J.; Lai, Y. Y.; Hsu, J. Y.; Cheng, S. W.; Hsu, C. S.; Cheng, Y. J. Synthesis of a 4,9-didodecyl angular-shaped naphthodiselenophene building block to achieve high-mobility transistors. *Chem. Mater.* **2016**, *28*, 5121–5130.
38 Planells, M.; Schroeder, B. C.; McCulloch, I. Effect of chalcogen atom substitution on the optoelectronic properties in cyclopentadithiophene polymers. *Macromolecules* **2014**, *47*, 5889–5894.
39 Ashraf, R. S.; Meager, I.; Nikolka, M.; Kirkus, M.; Planells, M.; Schroeder, B. C.; Holliday, S.; Hurhangee, M.; Nielsen, C. B.; Sirringhaus, H.; McCulloch, I. Chalcogenophene comonomer comparison in small band gap diketopyrrolopyrrole-based conjugated polymers for high-performing field-effect transistors and organic solar cells. *J. Am. Chem. Soc.* **2015**, *137*, 1314–1321.
40 Shi, S.; Tang, L.; Guo, H.; Uddin, M. A.; Wang, H.; Yang, K.; Liu, B.; Wang, Y.; Sun, H.; Woo, H. Y.; Guo, X. Bichalcogenophene imide-based homopolymers: chalcogen-atom effects on the optoelectronic property and device performance in organic thin-film transistors. *Macromolecules* **2019**, *52*, 7301–7312.
41 Kang, I.; An, T. K.; Hong, J. A.; Yun, H. J.; Kim, R.; Chung, D. S.; Park, C. E.; Kim, Y. H.; Kwon, S. K. Effect of selenophene in a DPP copolymer incorporating a vinyl group for high-performance organic field-effect transistors. *Adv. Mater.* **2013**, *25*, 524–528.
42 Shi, S.; Luo, J.; Wu, Z.; Liu, B.; Su, M.; Chen, P.; Zhang, X.; Feng, K.; Woo, H. Y.; Xiao, G. Fluorinated biselenophene-naphthalenediimide copolymers for efficient all-polymer solar cells. *Dyes Pigment* **2020**, *183*, 108721.
43 Noriega, R.; Rivnay, J.; Vandewal, K.; Koch, F. P.; Stingelin, N.; Smith, P.; Toney, M. F.; Salleo, A. A general relationship between disorder, aggregation and charge transport in conjugated polymers. *Nat. Mater.* **2013**, *12*, 1038–1044.
44 Tseng, H. R.; Phan, H.; Luo, C.; Wang, M.; Perez, L. A.; Patel, S. N.; Ying, L.; Kramer, E. J.; Nguyen, T. Q.; Bazan, G. C.; Heeger, A. J. High-mobility field-effect transistors fabricated with macroscopic aligned semiconducting polymers. *Adv. Mater.* **2014**, *26*, 2993–2998.
45 Lu, T.; Chen, F. Multiwfn: a multifunctional wavefunction analyzer. *J. Comput. Chem.* **2012**, *33*, 580–592.
46 Sirringhaus, H.; Brown, P. J.; Friend, R. H.; Nielsen, M. M.; Bechgaard, K.; Langeveld-Voss, B. M. W.; Spiering, A. J. H.; Janssen, R. A. J.; Meijer, E. W.; Herwig, P.; Leeuw, D. M. d. Two-dimensional charge transport in self-organized, high-mobility conjugated polymers. *Nature* **1999**, *401*, 685–688.

https://doi.org/10.1007/s10118-023-3026-z